

Towards optimal gas cooling with minimal aero-optical distortion for a laser amplifier head

Edward Lowell* and Oliver T. Schmidt†
University of California San Diego, La Jolla, California 92093

Frantisek Batysta‡, Issa Tamer§, and Thomas Spinka¶
Lawrence Livermore National Laboratory, Livermore, CA, 94550

Next-generation, high-peak-power, ultrashort-pulse lasers have the potential to efficiently deliver the high-average-power outputs required by many emerging technologies and areas of research. The combination of large size and low-repetition rates of previous-generation lasers make their effective and widespread usage impractical. The critical step in an effort to increase the repetition rate is a proper management of the waste heat generated in the laser gain medium. The current paper presents a computational approach with which to improve upon current gas-cooled amplifier designs; the ultimate goal being to optimize the head geometry for efficient cooling while maintaining minimal aero-optical distortion. This approach consists of several components, the focus of which are low-fidelity RANS simulations, and high-fidelity LES and aero-optical simulations. Preliminary results indicate that these components interface properly in handling the prescribed base case, and lay the groundwork for continued progress towards simulating, modeling, and optimizing the amplifier head for efficient cooling.

I. Introduction

The combination of energetic ($> 1J$) high-peak-power ultrashort laser pulses with high repetition rate, and therefore high average power, promises to enable new applications in laser-driven high-energy-density science, industry, and medicine. The most pressing technical issue for the next generation of solid-state lasers is thermal management. Typically, a gas cooled laser medium is split into several slabs, allowing for efficient heat removal from the slab faces by the cooling gas. Therefore, gas cooling is inherently an aperture- and average-power scalable technology that is utilized in several high energy laser systems to date [1, 2]. At Lawrence Livermore National Laboratory, the early development of this technology was led by Albrecht and Sutton, Albrechet et al., and Sutton et al. [3–6] and heat fluxes were of order $1W/cm^2$, and cooling efficiency was demonstrated up to $\sim 5W/cm^2$. Significant scaling (up to one order of magnitude) of this technology to higher extractable heat fluxes is required to enable the next generation of lasers. The tremendous requirements for removal of waste heat generated in the optical pumping process, combined with the necessity to maintain the highest optical beam quality, makes amplifier slab cooling of high-average-power solid-state lasers a formidable technological challenge at the intersection of heat transfer, fluid mechanics, and aero-optics.

In response to this challenge, the current work introduces a three-stage workflow consisting of low- and high-fidelity fluid simulations, and numerical aero-optical analyses. The final goal of this workflow is to optimize gas cooling within a laser amplifier head while maintaining minimal aero-optical distortion. Low-fidelity RANS simulations are used to obtain mean flow solutions and transition locations. High-fidelity LES simulations, informed by their RANS counterparts, provide solutions containing density fluctuations, which are then passed on to the aero-optical analysis. The aero-optical analysis provides insight into the optical quality of



Fig. 1 Gas-cooled laser head test stand.

*Ph.D. Student, Department of Mechanical and Aerospace Engineering

†Assistant Professor, Department of Mechanical and Aerospace Engineering, AIAA Member

‡Research Staff, Advanced Photon Technologies at NIF & Photon Science Directorate

§Research Staff, Advanced Photon Technologies at NIF & Photon Science Directorate

¶Program Element Leader for Laser Development, Advanced Photon Technologies at NIF & Photon Science Directorate

the laser beam passing through the flow found in the LES results. Section II will further outline these components, and section III will showcase preliminary results for this workflow with regards to handling an unheated base case.

II. Methodology

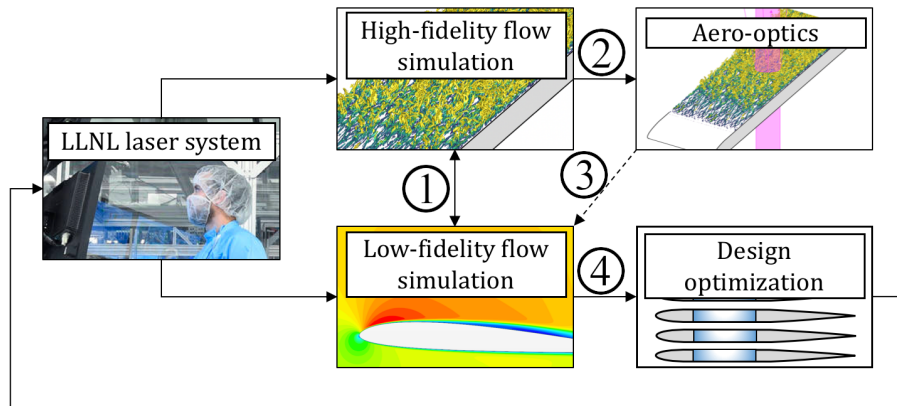


Fig. 2 Illustration of project workflow. Connections 1 and 2 bridge the gap between the low-fidelity RANS simulations and the aero-optics computations using high-fidelity LES. Connections 3 and 4 allow for the RANS simulations to be adjusted so that design optimization may be performed on the amplifier head. The current work focuses on connections 1 and 2.

The goal of this study is to optimize the cooling capability of a gas flow in a laser amplifier head under the constraint of maintaining minimal optical distortion. Having this goal in mind, the problem is approached with a workflow consisting of three main components:

- i Low-fidelity RANS simulations (Section II.A)
- ii High-fidelity LES simulations (Section II.B)
- iii Aero-optical analyses (Section II.C)

In consideration of design optimization, the low-fidelity RANS simulations have been selected due to their relatively low-computational costs. This allows for both fast simulations of simple domains, and simulations of larger and more complex geometries up to and including the entire amplifier head. However, by nature, the RANS simulations will not be able to produce solutions with the density fluctuations required for simulating a beam propagating through the flow. The high-fidelity LES component is introduced in order to bridge the gap between the low-fidelity RANS and the aero-optical analyses. Information from the RANS solutions (inlet conditions and transition location, for example) is used to inform the LES simulations. The solution from the LES is then passed on for proper aero-optical analysis on the fluctuating density field. In future work, the information from the aero-optics study will permit calibration of turbulence and heat-transfer models found in the low-fidelity RANS simulations for use in design optimization.

The current case focuses on a small section of a single channel within the laser amplifier head, as represented in Fig. 3. The RANS simulations will be conducted on the two-dimensional slice along the streamwise direction in the channel, while the LES simulation will consider the smaller three-dimensional segment within the channel. In addition to permitting calibration and fine-tuning of the interfaces between the components, this focus has allowed for initial studies to be conducted on this base case.

A. Reynolds-Averaged Navier-Stokes simulation (RANS)

The low-fidelity component of this study makes extensive use of RANS simulations, where the k- ω Turbulence Model is applied to determine the solution for a completely turbulent flow. Assumptions made in this part of the study reinforce its low-fidelity and low-computational cost objectives. Here, the flow is assumed to be two-dimensional and incompressible, where the steady-state solution is of interest. The assumption for two-dimensional flow is based off of the large aspect ratio found in any $y - z$ aligned cross-section of the channel, where the aspect ratios are found to be on the order of 100. The reasoning behind this assumption is that the main region of interest, the laser gain medium, lies at a sufficient distance away from the sidewalls of the channel such that the flow near these walls will have negligible

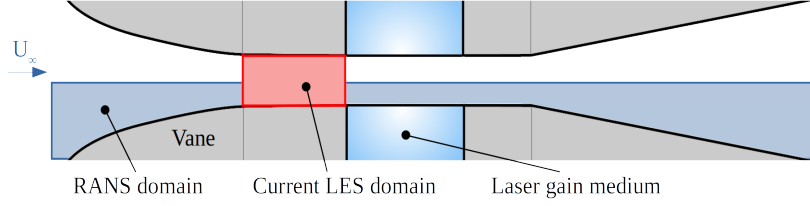


Fig. 3 Illustration of the $x - y$ cross-section of a single channel formed by two half-vanes. The 2D RANS domain utilized symmetry along the centerline, while the 3D LES domain simulates the entire width of the channel, and uses the RANS solution for informing inlet and outlet conditions. (Schematic not to scale.)

impact on the flow over the gain medium. Thus, a two-dimensional slice of the flow in the amplifier head would be a reasonable, low-fidelity representation of a majority of the domain. The incompressibility assumption is based on the flow consisting of helium gas at 273 K, which corresponds to a speed of sound of approximately 973 m/s. It was expected that the maximum velocity in the channel would reach somewhere between 100 and 200 m/s, yielding a maximum Mach number that ranges from 0.1 to 0.2.

In this study, COMSOL Multiphysics® is used to simulate fully turbulent flow using its implementation of the k-omega turbulence model [7].

B. Large-eddy simulation (LES)

In contrast to the assumptions made in the low-fidelity component, the assumptions made in the high-fidelity component are tailored towards linking the LES solutions to an aero-optical analysis. The main assumptions for the current case are that of compressible, three-dimensional flow of an ideal gas. The ideal gas assumption is based on the flow being composed of helium gas with reference values as shown in Table 1. At the specified reference values, the compressibility factor of helium gas is close to 1, indicating that the ideal gas assumption is suitable [8]. In keeping with the high-fidelity aspect of this portion of the study, the full, three-dimensional compressible flow equations are solved using Cascade Technologies' compressible flow solver, CharLES [9]. CharLES's implementation of the Vreman subgrid scale model was selected to account for the unresolved turbulence. For the computational domain, periodicity is utilized in the spanwise direction in order to allow for a comparison to the RANS solution, as well as to reduce computational cost. This periodicity assumption has similar implications as those of the two-dimensional assumption in the low-fidelity component; that is to say the solutions will represent the flow far from any side-wall effects.

C. Aero-optics

The concept of face-cooled laser medium involves the laser beam propagating through both the active laser gain medium and through the turbulent gas coolant flowing in the channel. As the turbulent gas flow extracts the heat from the walls of the channel, its instantaneous refractive index will vary through the computational domain due to temperature and pressure perturbations. In turn, density fluctuations due to these perturbations will cause optical aberration to the laser beam. A numerical analysis of the effect of the fluctuating density field on optical aberration is conducted in the third component of this study.

To assess the optical aberrations caused by the heated turbulent flow, we model a propagation of a coherent beam in a medium with variable refractive index using tools of Fourier optics [10]. The numerical propagation of a laser beam in free space from the input plane at $Z = 0$ to the output plane at $Z = L$ in a free space is given by an amplitude transfer function in a frequency domain

$$A_L(f_x, f_y) = \mathcal{H}_L(f_x, f_y) \cdot A_0(f_x, f_y), \quad (1)$$

where spectral amplitude A is calculated from the scalar amplitude of the electric field using a 2D Fourier transform at the selected plane.

$$A_z(f_x, f_y) = \iint_{-\infty}^{+\infty} U_z(x, y) \exp\{-2i\pi(f_x x + f_y y)\} dx dy \quad (2)$$

Because the refractive index of helium is close to unity and the aberrations are expected to be small, we expect that most of the scattered laser energy will still propagate almost parallel to the optical axis. Hence, we can use a paraxial Fresnel

approximation and use the spectral amplitude transfer functions as follows:

$$\mathcal{H}_L(f_x, f_y) = \exp\left\{-i\pi \frac{L}{\lambda} \cdot (f_x^2 + f_y^2)\right\}, \quad (3)$$

where λ is a vacuum wavelength; f_x , and f_y are spatial frequencies.

The refractive index of the gas varies proportionally with the density as shown in equation

$$n - 1 = (n_{\text{sta}} - 1) \frac{\rho}{\rho_{\text{sta}}}, \quad (4)$$

where n is the refractive index of the gas, ρ is its density, and $n_{\text{sta}}, \rho_{\text{sta}}$ is a standard refractive index and density at a pressure of 1 bar and a temperature of 0 °C.

Numerically, the effect of the variable phase distortions is accounted for iteratively. The total propagation distance is split into N slices. Instead of solving the Maxwell's equations in the inhomogenous medium, the phase aberrations in each slice are accounted for at the beginning of each slice, followed by a free space propagation to the next slice. The iterative equation propagating the beam between the k -th and $(k + 1)$ -th slice is given as follows

$$U_{k+1} = \mathcal{I} \mathcal{F} \mathcal{T} \left[\mathcal{H}_{\frac{L}{N}} \cdot \mathcal{F} \mathcal{T} \{U_k \exp\{-i\phi_k\}\} \right], \quad (5)$$

where

$$\phi_k(x, y) = \frac{2\pi}{\lambda} \Delta n(x, y) \frac{L}{N}, \quad \Delta n(x, y) = n(x, y) - \bar{n}, \quad (6)$$

where \bar{n} is a domain average of the refractive index.

III. Preliminary Results

A. Low-fidelity simulations

The x-velocity and pressure fields within the relevant, straight-channel region are shown in conjunction with their LES counterparts in Fig. 7. Though the location of transition in the base case is not yet verified, a turbulent flow will ultimately be desired due to its greater capacity for heat removal and its potential for lower optical distortion. With this consideration in mind, the base channel domain was assumed to be fully turbulent, and was solved in COMSOL using the k-omega turbulence model. Boundary conditions consisted of a mass-flow inlet, a pressure outlet, adiabatic channel walls, and symmetry elsewhere. The inlet mass-flow rate was chosen such that the inlet had an average velocity of 20 m/s, with a turbulence intensity of 5%.

B. High-fidelity simulations

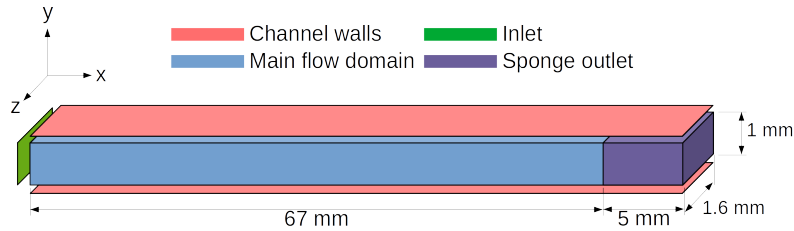


Fig. 4 Dimensions and boundary conditions for LES domain.

1. Initial conditions

The LES was conducted on the domain shown in Fig. 4. The steady-state solution of the low-fidelity RANS case was used as the initial condition for the high-fidelity LES. The two-dimensional RANS solutions for velocity, pressure, and temperature were extended into a three-dimensional solution by assuming the profiles were uniform in the spanwise direction. It should be noted that, since the RANS workflow assumed the flow was incompressible, the temperature profile was constant and set to the reference temperature for the helium gas. The two-dimensional profiles can be seen further down in section 7, where the steady-state RANS and LES solutions are compared.

Table 1 LES reference values for Helium gas

Property	Reference value	Units
Density, ρ	0.714	kg/m ³
Temperature, T	273.15	K
Pressure, p	4.035×10^5	Pa
Viscosity, μ	2.0×10^{-5}	Pa·s
Specific heat ratio, γ	5/3	-

Table 2 LES boundary condition summary

Boundary	Condition	Properties
Inlet	Turbulent Inlet	See Fig. 5
Outlet	Sponge	$p = 407,745$ Pa
Channel Walls	Adiabatic, no-slip	Algebraic wall-model
Spanwise Extents	Periodic	—

2. Boundary conditions

In order to maintain simplicity for initial headway into this study, a section of the straight portion of the channel was simulated, as represented in Fig. 3, and detailed in Fig. 4. A summary of the boundary conditions can be seen in Table 2. The inflow condition is CharLES' implementation of a synthetic turbulent boundary condition. The profiles of velocity, temperature, pressure, and turbulence kinetic energy were taken from the corresponding location of the fully turbulent RANS case, and are used to inform the LES inlet. An algebraic wall-model was applied at the walls, and it was assumed the walls are adiabatic and satisfy no-slip. A sponge region was applied at exit of the domain in order to minimize spurious reflections. The sponge pressure corresponds to the pressure found in the equivalent location in the RANS case.

3. Solution and comparison to RANS

A cross-section along the $x - y$ plane of the instantaneous solution at 300,000 timesteps is shown in Fig. 6. Note that for clarity, the domain does not extend to the full streamwise length. The final snapshot of the LES containing the temporally averaged data was compared to the corresponding RANS steady-state solution. Reduction of the 3D LES solution to 2D was conducted by taking the mean of the flow in the spanwise direction. The results of this reduction, in addition to the RANS solution and difference between solutions, can be seen in Fig. 7. The differences between the RANS and LES solutions for both velocity and pressure appear to be minimal for the majority of the domain. However, it is clear that the flow towards the inlet, and near the walls tend to exhibit the most disparity. This is attributed to the difference in boundary condition handling between the two solvers. While the RANS solution resolved the flow near the wall, the LES utilized wall-models. This is evident in Fig. 8, where the wall-normal flow profiles are compared at different streamwise locations. In addition to the slight discrepancy in the wall boundary conditions, the flow near the inlet shows some disparity between the RANS and LES solutions, as is evident in Fig. 7a. This is attributed to the synthetic turbulence generated at the inlet of the LES requiring adequate distance to become physically realizable.

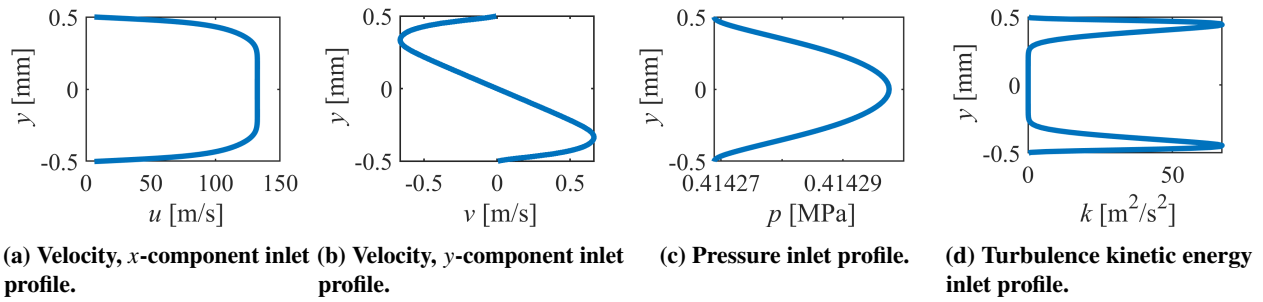


Fig. 5 Inlet profiles from the 2D RANS steady-state solution used to inform the 3D LES. These profiles were extruded in the spanwise direction for conversion to 3D. Note that the velocity z -component and temperature are considered constants; 0 m/s and 273.15 K, respectively.

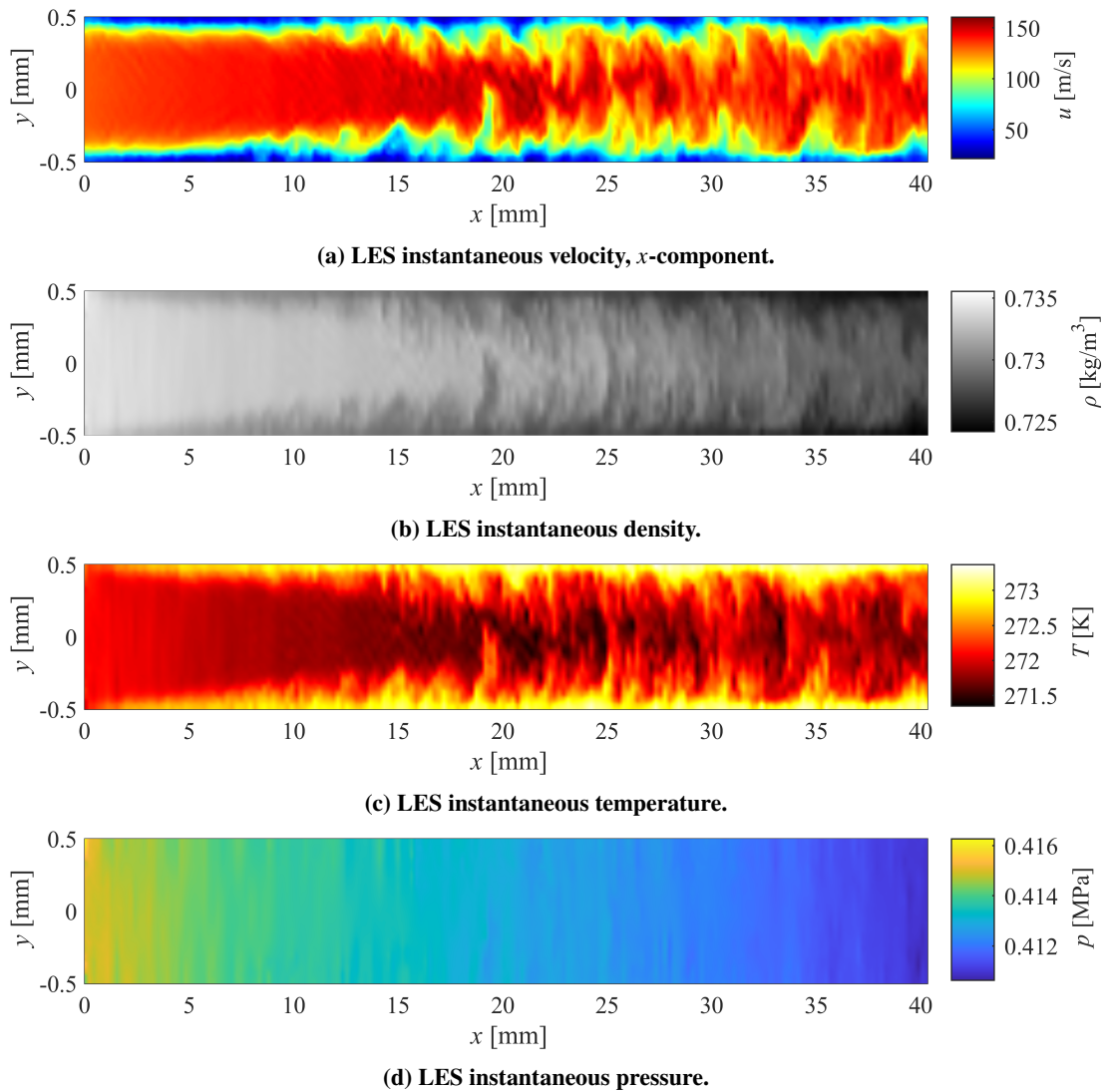
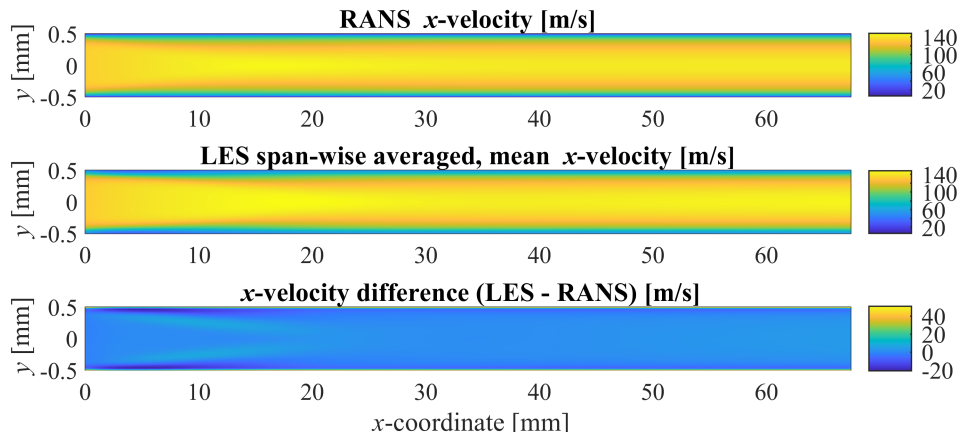
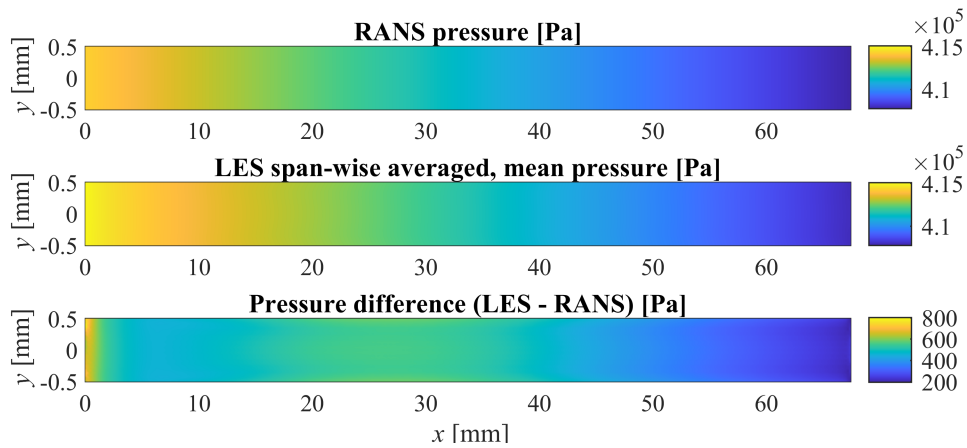


Fig. 6 LES instantaneous solution at 6.5 ms after 300,000 timesteps. Note that, for clarity, the domain does not span the entire streamwise length.



(a) Comparison of RANS and LES steady-state solutions for the velocity, x -component.



(b) Comparison of RANS and LES steady-state solutions for pressure.

Fig. 7 Comparison of RANS steady-state solution to the spanwise- and time-averaged LES solution. Each subplot contains the RANS solution of the selected flow variable, the "span-averaged, temporal-mean" LES solution, and a difference between the two solutions.

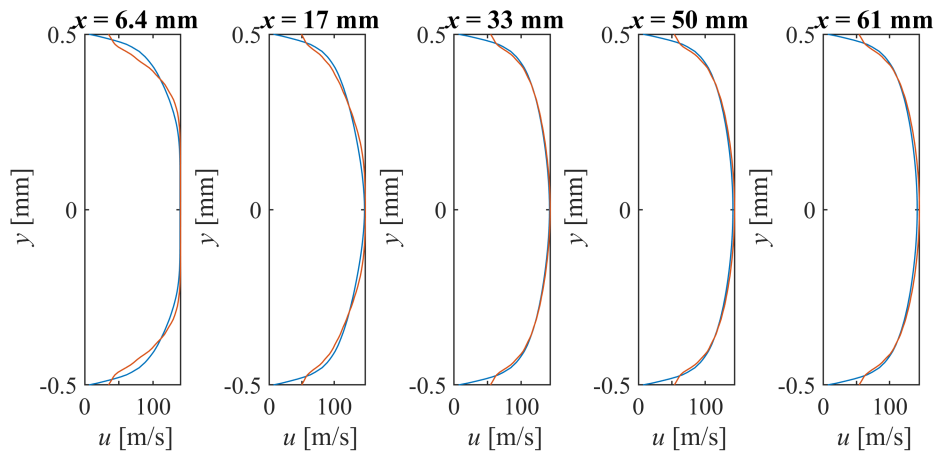
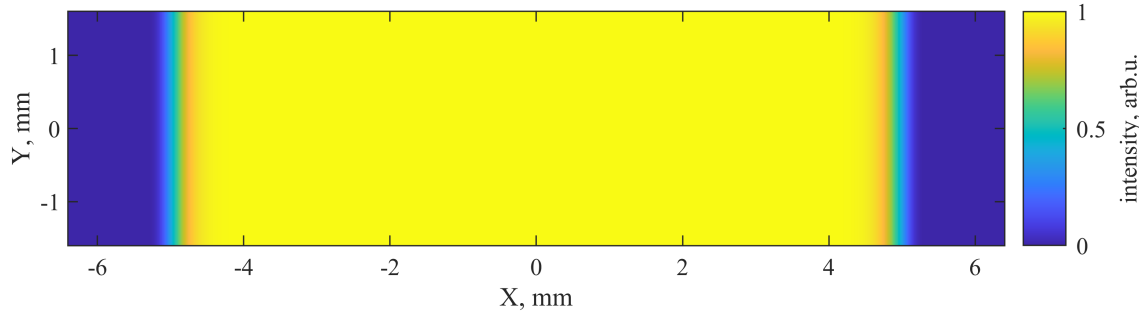
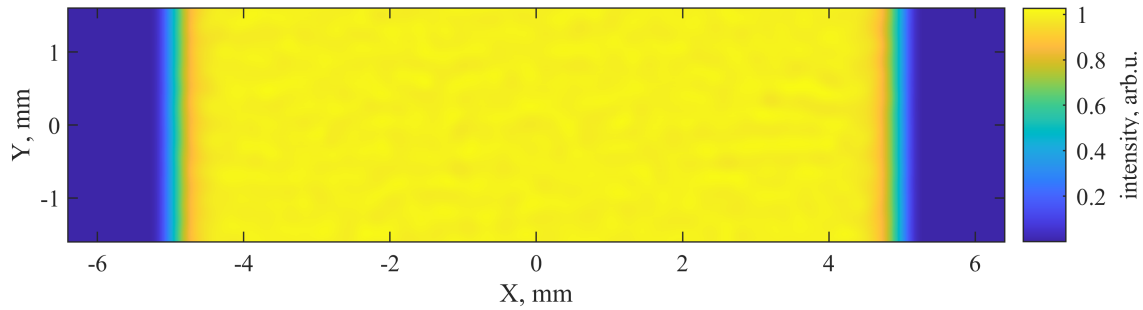


Fig. 8 Comparison between the velocity x -component profiles of the 2D, steady-state RANS solution to those of the spanwise-averaged, temporal mean LES solution. These profiles are taken at the specified x -coordinates, where the blue curves represent the RANS profiles, and the red curves represent the LES profiles.



(a) Input beam intensity profile..



(b) Output beam intensity profile.

Fig. 9 Beam profiles before and after propagation in Y through the equivalent of around 20 repeated density fields from the LES simulation.

C. Aero-optics

The variations in the index of refraction are proportional to the gas density, and were used to propagate the beam through the gas, where Fourier optics formalism was used for calculation. The initial beam intensity can be seen in Fig. 9a. Note the coordinate system change between the flow and optics sense. The coordinates for the flow, x , y , and z correspond to the optical coordinates, X , $-Z$, and Y , respectively. The initial beam was numerically propagated in the wall-normal direction through the flow about 20 times in order to simulate the beam passing through multiple channels. The final beam intensity profile after propagation is shown in Fig. 9b.

In the turbulent flow, losses in the laser beam are attributed to optical scattering - that is the energy that appears to be propagating at different angles than that of the original beam. The scattered energy in the Fourier domain was integrated, and the conclusion is that the scattering losses for this demonstration are negligible – around 0.03% of energy is lost due to scattering. This minimal loss is attributed to the refractive index of Helium being favorably close to 1. It is expected that the addition of proper boundary conditions for surface heating will contribute to increased temperature and density fluctuations, further influencing optical distortion when compared to this base case.

IV. Outlook

The currently presented study emphasizes the interfacing between the RANS, LES, and aero-optical components. Preliminary results show that the RANS and LES components yield corresponding solutions. And, as expected, the aero-optics simulation revealed minimal scattering in the unheated base case. While focus has been on a small segment of the channel, the flexibility of the components and their interfacing allow for easy expansion to larger domains. Ongoing work includes expansion of the RANS domain to the full heater head, and applying transition models so that transition locations can be obtained. In addition the LES domain is to be extended to the full channel length, where proper boundary conditions for the heated surface will be implemented.

Acknowledgments

OTS and EL gratefully acknowledge support by the U.S. Department of Energy under FES Award DE-SC0021339 (PM Kramer Akli). The aero-optics work reported in this study was performed under the auspices of the U.S. Department of Energy by Lawrence Livermore National Laboratory under Contract DE-AC52-07NA27344. Information presented in this report pertaining to said work has been approved for release under LLNL-PROC-834549.

References

- [1] Haefner, C., Bayramian, A., Betts, S., Bopp, R., Buck, S., Cupal, J., Drouin, M., Erlandson, A., Horáček, J., Horner, J., et al., “High average power, diode pumped petawatt laser systems: a new generation of lasers enabling precision science and commercial applications,” *Research Using Extreme Light: Entering New Frontiers with Petawatt-Class Lasers III*, Vol. 10241, International Society for Optics and Photonics, 2017, p. 1024102.
- [2] Mason, P., Divoký, M., Ertel, K., Pilař, J., Butcher, T., Hanuš, M., Banerjee, S., Phillips, J., Smith, J., De Vido, M., et al., “Kilowatt average power 100 J-level diode pumped solid state laser,” *Optica*, Vol. 4, No. 4, 2017, pp. 438–439.
- [3] Albrecht, G., and Sutton, S., “Gas cooling of laser disks,” *Energy Technol. Rev.*, 1988.
- [4] Albrecht, G. F., Sutton, S. B., Robey, H. F., and Freitas, B. L., “Flow, heat transfer, and wavefront distortion in a gas cooled disk amplifier,” *High Power and Solid State Lasers II*, Vol. 1040, International Society for Optics and Photonics, 1989, pp. 37–55.
- [5] Albrecht, G. F., Robey, H. F., and Erlandson, A. C., “Optical properties of turbulent channel flow,” *Applied optics*, Vol. 29, No. 21, 1990, pp. 3079–3087.
- [6] Sutton, S., Albrecht, G., and Robey, H., “Heat removal in a gas cooled solid-state laser disk amplifier,” *AIAA journal*, Vol. 30, No. 2, 1992, pp. 431–435.
- [7] COMSOL, “COMSOL Multiphysics® v. 5.6.” www.comsol.com, COMSOL AB, Stockholm, Sweden.
- [8] Stroud, L., Miller, J. E., and Brandt, L. W., “Compressibility of Helium at-10° to 130° F. and Pressures to 4000 PSIA,” *Journal of Chemical and engineering Data*, Vol. 5, No. 1, 1960, pp. 51–52.
- [9] Brès, G. A., Ham, F. E., Nichols, J. W., and Lele, S. K., “Unstructured large-eddy simulations of supersonic jets,” *AIAA journal*, Vol. 55, No. 4, 2017, pp. 1164–1184.
- [10] Goodman, J. W., “Introduction to Fourier optics. 3rd,” *Roberts and Company Publishers*, 2005.